

# Production of massless charm jets in $pp$ collisions at next-to-leading order of QCD in comparison with CMS data

Gustav Kramer\*

*II. Institut für Theoretische Physik, Universität Hamburg,  
Luruper Chaussee 149, 22761 Hamburg, Germany*

(Dated: October 28, 2020)

## Abstract

We present predictions for the inclusive production of charm jets in proton-proton collisions at 2.76 and 5.02 TeV. The charm-quark is considered massless. In this scheme we find that the ratio of the next-to-leading order to the leading order cross section (K factor) is almost equal to one depending essentially on the choice of the renormalization and factorization scale. Adding non-perturbative corections obtained from Pythia Monte Carlo calculations lead to resonable agreement with experimental c-jet cross sections obtained by the CMS [10] collaboration.

---

\*Electronic address: [gustav.kramer@desy.de](mailto:gustav.kramer@desy.de)

## I. INTRODUCTION

The cross-section for producing jets in pp collisions at the Large Hadron Collider (LHC) yields an important testing field of perturbative Quantum Chromodynamics (QCD) and offers the possibility to learn more about proton-parton distributions (PDFs). So far most of the predictions for LHC experiments have been done for the sum of ingoing mass less quarks up to b quarks. They have been found in very good agreement with the measurements. In these predictions, the contributions of heavy quarks (charm and bottom) constitute only a few percent of the total production cross-sections. Considering the experimental data, from these comparisons it is not clear whether the heavy quark jets are satisfactorily described by perturbative QCD (pQCD) calculations.

So far, most of the predictions for heavy-quark jets separately have been done in the massive quark scheme or fixed-flavor-number scheme (FFNS) [1, 2] in which heavy quarks appear in the final-state only and not as partons in the initial state, as for example in the zero-mass variable-flavor-number scheme (ZM-VFNS). In this scheme the calculations for the sum of all flavors have been done. This is also the appropriate scheme for most of the PDF parametrizations of the proton. A few years ago we have presented predictions of massless charm [3] and bottom jets [4] in  $p\bar{p}$  and  $pp$  collisions at next-to-leading order (NLO). In particular, in the latter reference, we have compared our predictions for bottom jets in  $p\bar{p}$  collisions at  $\sqrt{S} = 1.96$  TeV and  $pp$  collisions at  $\sqrt{S} = 7$  TeV. The measurements, we have been compared to, have been done by the CDF collaboration [5–7] at the Tevatron and by the CMS collaboration [8] at the LHC. At the LHC also the ATLAS collaboration has measured inclusive b-jet cross section at  $\sqrt{S} = 7$  TeV [9], to which we have not compared our results, however.

In our work [4] we have found that at small transverse momentum  $p_T$  of the bottom jets the ratio of the NLO to the leading-order (LO) cross section is smaller than one. It increases with increasing  $p_T$  and approaches one at larger  $p_T$  at a value depending essentially on the choice of the renormalization scale. Adding non-perturbative corrections obtained from PYTHIA Monte Carlo computations which contain in addition to the LO perturbative contributions the hadronic and parton shower corrections, we obtained reasonable agreement with the experimental b-jet across sections as measured by the CMS collaboration [8].

At the time of our earlier work [4] data about charm-jet production, neither from CDF

nor by one of the LHC experiments were not available, presumably since the experimental identification of charm jets is much more difficult than for bottom-jets. Therefore we have not checked whether our findings for bottom-jet in [4] is also true for the production of charm-jets. This is the purpose of this work, since very recently, experimental data about single-inclusive charm-jet cross section have become available as presented by the CMS collaboration [10] at the LHC. These cross-section have been measured for two  $\sqrt{S}$  values,  $\sqrt{S} = 2.76$  TeV and  $\sqrt{S} = 5.02$  TeV for the rapidity region  $|y| < 2.0$  and for five  $p_T$  bins in the range  $40 < p_T < 250$  GeV (in the case of the  $\sqrt{S} = 2.76$  TeV) and for  $80 < p_T < 400$  GeV (for the case  $\sqrt{S} = 5.02$  TeV). We have calculated the cross-section for the same  $p_T$  bins as in the CMS experiment and the same rapidity ( $y$ ) bin for both center-of-mass energies.

In Sec. 2 we describe the PDF input and outline the theoretical framework. Section 3 contains our results for single-inclusive charm-jet cross-sections  $d\sigma/dp_T$  and the comparison with the cross-section measured by the CMC collaboration. A summary and some conclusions are presented in Sect. 4.

## II. PDF INPUT AND THEORETICAL FRAMEWORK

As in our earlier publications on charm jets [3] and bottom jets [4] we rely on previous work on dijet production in the process  $\gamma + p \rightarrow jet + X$  [11, 12] in which cross-sections for inclusive one-jet and two-jet production up to NLO for both, the direct and the resolved contributions, are calculated. The resolved part of this routine can be used for  $pp$  collisions replacing the photon PDF by the proton PDF. The routine [11, 12] contains quarks of all flavors up to and including the bottom quark as well as the gluon. In this work about charm jets the bottom quark will be excluded. The routine has been modified in such a way that at least one charm quark appears in the final state in the same way as we did for charm jets in Ref. [3].

The routine [11, 12] is based on massless quarks, i.e. the charm quark is also assumed massless. This is justified as the transverse momentum  $p_T$  of the produced charm jet is large enough, i.e.  $p_T \gg m_c^2$ , which is the case for the two data sets of CMS in [10].

For our predictions of the inclusive c-jet cross-section we employ the MSTW 2008 NLO [13] PDF (central value) of the Durham collaboration as we did in our earlier work for bottom jets [4]. The chosen asymptotic scale parameter  $\Lambda_{\overline{MS}}^{(5)} = 0.226$  GeV corresponds to

$\alpha_s^{(5)}(m_Z) = 0.118$ . The  $\Lambda_{\overline{MS}}^{(5)}$  is adjusted to the appropriate  $\Lambda_{\overline{MS}}^{(4)}$  value for calculating charm. We shall also check for comparison two more modern PDF sets, namely CT14 [14] and MHSW [15]. The center-of mass energy of the proton-proton collisions is taken  $\sqrt{S} = 2.76$  and  $\sqrt{S} = 5.02$  TeV as in the CMS data sets. The comparison of results for the different PDFs is done only for  $\sqrt{S} = 5.02$  TeV. We choose the renormalization scale  $\mu_R = \xi_R p_T$  and the factorization scale  $\mu_F = \xi_F p_T$  where  $p_T$  is the largest transverse momentum of the two or three final state jets.  $\xi_R$  and  $\xi_F$  are dimensionless scale factors, which are varied around  $\xi_R = \xi_F$  to be specified later.

### III. RESULTS AND COMPARISON WITH CMS DATA

As a check of our program we have already calculated the cross-section  $d\sigma/dpp_T dy$  for  $pp \rightarrow \text{single jet} + X$  for  $\sqrt{S} = 7$  TeV in the  $p_T$  region  $18 \leq p_T \leq 1684$  GeV and in the rapidity region  $|y| \leq 0.5$  and compared to CMS data [16] in  $p_T$  bins as chosen by CMS [16]. Nonperturbative (NP) corrections for hadronization and multiple parton interactions were estimated by CMS [16] and are published in the Durham Hep Data project [17]. They are applied to the NLO perturbative QCD predictions. These corrected inclusive jet cross-sections including the theoretical error together with the CMS data are shown in Fig. 1 of our work [3]. The agreement between data and the theoretical prediction shown there is quite good. The PDF used in this comparison was CT10 [18]. Concerning the charm-jet calculation we have first calculated the inclusive cross-section  $d\sigma/dp_T$  integrated over  $|y| \leq 2.0$  for  $\sqrt{S} = 5.02$  TeV in LO pQCD for the five  $p_T$  bins as in the CMS paper [10]. The scales for the LO cross-section are chosen as  $\xi_R = \xi_F = 1.0$  (default solid line histogram in Fig.1, left side),  $\xi_R = \xi_F = 0.50$  (upper dashed line histogram in Fig 1, left side) and  $\xi_R = \xi_F = 2.0$  (lower dashed line histogram in Fig 1, left side) following our previous work [4]. These three calculations are compared to the inclusive charm-jet cross-section in Fig. 1, left side for the same  $\sqrt{S}$ . These theoretical LO cross-sections are not corrected for NP effects. In addition, in the right frame of Fig. 1 we show the K factor, the ratio of the NLO to the LO cross-section, where  $K = (d\sigma/dp_T)_{NLO}/(d\sigma/dp_T)_{LO}$  as a function of  $p_T$  for the five  $p_T$  bins as in the CMS data for  $\sqrt{S} = 5.02$  TeV and for the same scale choices as in the left frame of Fig. 1. The NLO cross-section in the denominator is calculated with the scale  $p_T$  and is used for the ratio with the three LO cross-section. As we shall see later

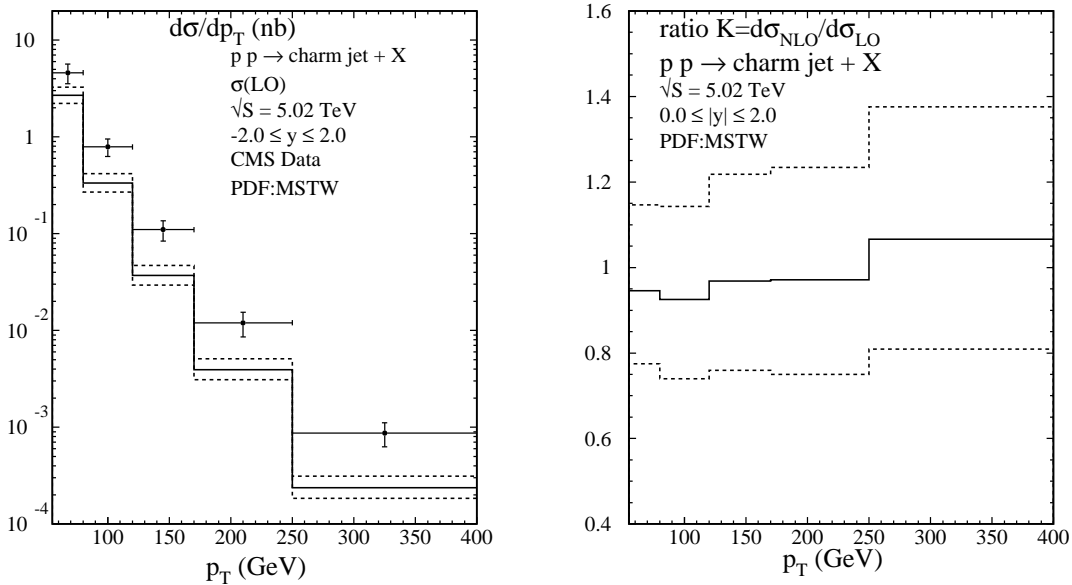


FIG. 1: Left side: single-inclusive c-jet cross section in LO as a function of  $p_T$  integrated over the rapidity region  $0.0 \leq |y| \leq 2.0$  compared to CMS data [10], which are the points with error bars. The LO theoretical predictions are not corrected by non-perturbative effects via a multiplicative factors. The theoretical error (dashed lines) is obtained by scale variation as given in the text. The solid line indicates the default scale choice. Right side: Ratio of single-inclusive c-jet cross section in NLO and LO integrated over rapidity in the region  $0.0 \leq |y| \leq 2.0$  as a function of  $p_T$  for three scale choices as given in the text.

the NLO cross-section depends much less on the choice of scales. In the left frame these cross section results are compared to the measured CMS values [10]. As we can see, the calculated LO cross-sections are smaller than the data by approximately a factor of 1.8 for the lowest  $p_T$  bin and a factor 3.7 for the largest  $p_T$  bin. For jet cross-sections of all flavors, the NLO corrections usually increase the corresponding LO cross sections by factors 2 to 3. If this would be the case also for three c-jet cross-sections we would have approximate agreement with the data. The corresponding K factor is shown in Fig. 1 (right frame). It is approximately equal to  $1.0 \pm 0.3$ . The error is due to the scale dependence of the LO cross-section  $d\sigma/dp_T$ . It is nearly constant as a function of  $p_T$ . This is in contrast to the b-jet production K factor in Ref. [4], which increased from 0.6 to 1.2 in the same  $p_T$  range as for the c-jet cross-section  $d\sigma/dp_T$ . Results for  $\sqrt{S} = 2.76$  TeV, not shown in this work,

are expected to look similar.

Next, we want to show, how our NLO predictions describe the CMS c-jet cross-section data [10]. For this comparison we need the non-perturbative corrections. For this we take the PYTHIA prediction also contained in Ref. [10] for  $\sqrt{S} = 2.76$  TeV and  $\sqrt{S} = 5.02$  TeV. Unfortunately these predictions are not given in numerical form. So, we read them from Fig. 6 (upper and lower frame) in Ref. [10]. Although errors for these cross-sections are shown in these figures also, it is difficult to obtain them from the figures. From the PYTHIA cross sections calculated by CMS from the PYTHIA routine we subtract our LO predictions with the scale choice  $\xi_R = \xi_F = 1.0$ . The result is shown in Fig. 2 (left frame) for  $\sqrt{S} = 2.76$  TeV and in Fig. 3 (left frame) for  $\sqrt{S} = 5.02$  TeV as dotted histograms. In these two figures we show also the two CMS data sets for the two center-of-mass energies and the corresponding NLO predictions for  $d\sigma/d_T$  for the respective  $p_T$  bins and in the rapidity range  $|y| \leq 2.0$  as for the CMS data. These predictions are shown for three scale choices (full histogram for default, upper and lower dashed histograms for maximal and minimal cross sections). The selection of these scales was performed as follows. First we calculated the NLO cross sections for both  $\sqrt{S}$  values by varying the scales according to the following combinations of  $\xi_R$  and  $\xi_F$ : (1,1), (1,2), (2,1), (2,2), (1/2,1), (1,1/2) and (1/2,1/2). The largest up and down cross-sections for these choices are taken as the scale variation. The default cross-section is taken as the middle value of the maximal and the minimal cross-section out of these seven scale choices. It is found that the changes of these cross-sections between the maximal and minimal scale choices are rather small, and much smaller than in the LO predictions. This is understandable because of the well-known compensation of scale errors in the NLO case. Our main results are shown in Fig. 2  $\sqrt{S} = 2.76$  TeV and Fig. 3  $\sqrt{S} = 5.02$  TeV, respectively. In the left frame of these two figures we show our result for the NLO cross sections  $d\sigma/dp_T$  for the five  $p_T$  bins and  $|y| \leq 2.0$  for the two  $\sqrt{S}$  values, respectively, together with the corresponding CMS [10] data for these cross sections and the ‘‘PYTHIA’’ cross section  $d\sigma/dp_T$  read from Fig. 6 of Ref. [10] minus the LO cross section  $d\sigma/dp_T$  for the default scale with  $\xi_R = \xi_F = 1.0$  as the dotted histogram. We observe that the NLO cross-section values in Fig. 3. (left frame) differ only little from the corresponding LO cross section value. This we should have expected from the K factor shown in Fig. 1 (right frame). In addition, we observe that the theoretical error due to the scale variations is very much reduced in the NLO predictions in Fig. 3 (left frame) when compared to the LO

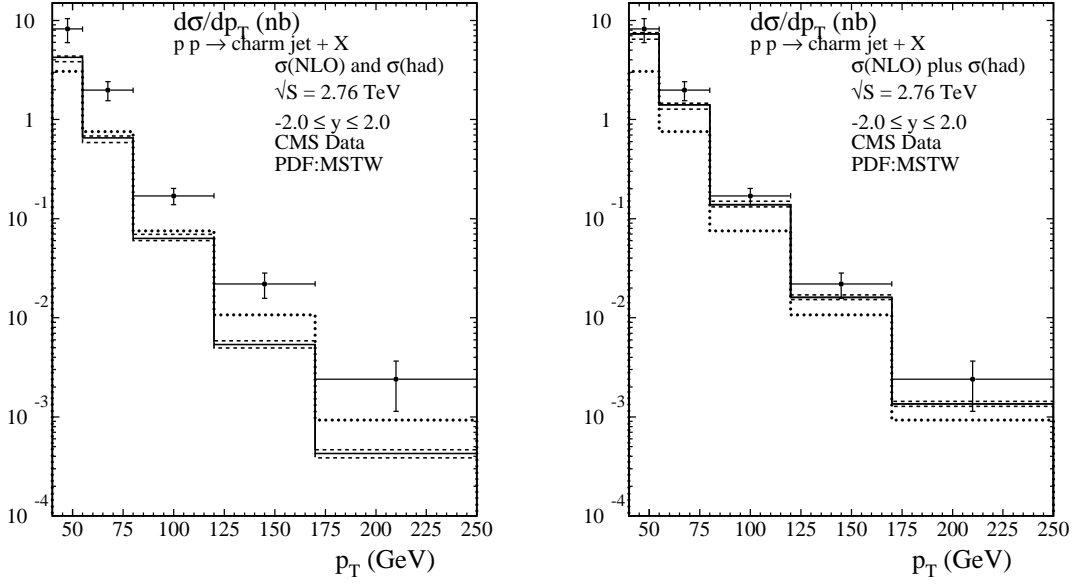


FIG. 2: Left side: Single-inclusive c-jet cross-section in NLO as a function of  $p_T$  integrated over the rapidity region  $0.0 \leq |y| \leq 2.0$  at  $\sqrt{S} = 2.76$  TeV compared to CMS data [10], given by the full line histogram and points with error bars. The NLO theoretical predictions is not corrected by non-perturbative effects via multiplicative factors. The theoretical error (dashed histograms) is obtained by scale variation as given in the text. The solid histogram indicates the default scale choice. The dotted histogram is the PYTHIA minus LO prediction. Right side: Single-inclusive c-jet cross-section in NLO plus the PYTHIA minus LO prediction as a function of  $p_T$  integrated over the rapidity region  $0.0 \leq |y| \leq 2.0$  compared to CMS data [10], given by the full lines and points with error bars.

predictions in Fig. 1 (left frame). The next step is to add the PYTHIA cross-section minus the LO cross-section to the NLO theoretical cross section as given by the dotted histogram. The result can be seen in Fig. 2 and 3 (right frame), respectively. As is seen, we obtain rather good agreement between our prediction including non-perturbative correction and our NLO predictions for  $d\sigma/d_T$ . In Fig. 2 (right frame) at  $\sqrt{S} = 2.76$  TeV for four  $p_T$  bin cross-sections  $d\sigma/dp_T$  (out of five) we have agreement inside the experimental errors and in Fig. 3 (right frame) all five  $p_T$  bin cross-sections  $d\sigma/dp_T$  agree with the CMS data inside the experimental accuracy. This agreement is not unexpected. In the CMS publication [10] it was shown that the measured cross-section  $d\sigma/dp_T$  for both center-of-mass energies agree

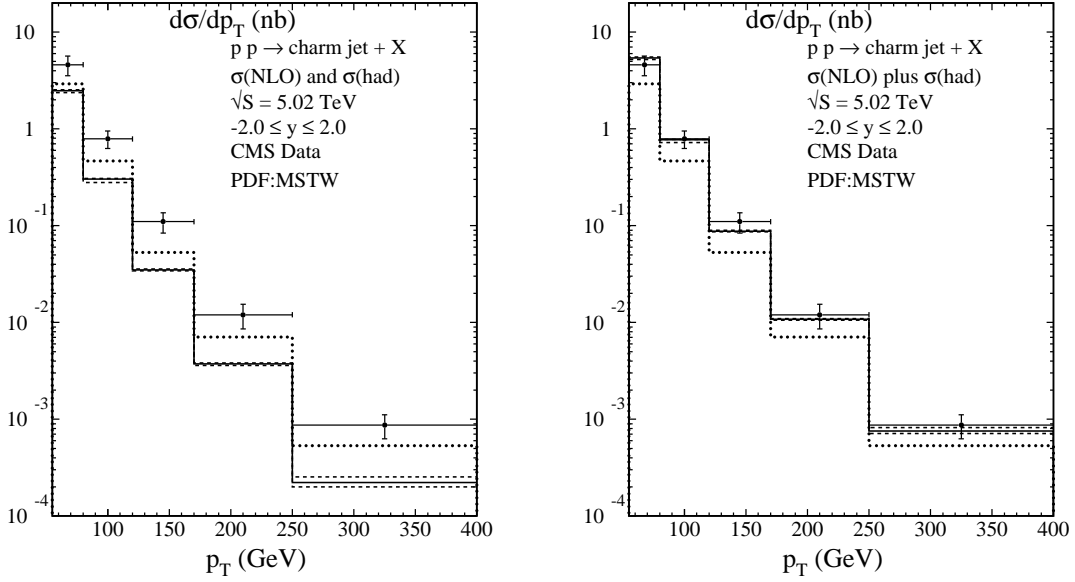


FIG. 3: Left side: Single-inclusive c-jet cross-section in NLO as a function of  $p_T$  integrated over the rapidity region  $0.0 \leq |y| \leq 2.0$  at  $\sqrt{S} = 5.02$  TeV compared to CMS data [10], given by the full line histogram and points with error bars. The NLO theoretical predictions is not corrected by non-perturbative effects via multiplicative factors. The theoretical error (dashed histograms) is obtained by scale variation as given in the text. The solid histogram indicates the default scale choice. The dotted histogram is the PYTHIA minus LO prediction. Right side: Single-inclusive c-jet cross-section in NLO plus the PYTHIA minus LO prediction as a function of  $p_T$  integrated over the rapidity region  $0.0 \leq |y| \leq 2.0$  compared to CMS data [10], given by the solid lines and points with error bars.

quite well with the PYTHIA 6.424 [19], tune Z2 [20] prediction. In our results shown in Fig. 2 and Fig. 3 (right frame), respectively, the LO cross section contained in PYTHIA 6 is just replaced by our NLO  $d\sigma/dp_T$ . Since they are almost equal as shown in Fig. 1, (right frame) it is clear that our prediction of the NLO cross section plus the hadronic correction taken from PHYTHA must agree with the CMS data. In order to account for a possible scale dependence of the PYTHIA minus LO cross section we have in Fig. 2 and Fig. 3 (right frame) doubled the theoretical error due to scale variation obtained in the NLO cross-section. As is seen in Fig. 2 (left frame) and Fig. 3 (left frame) the correction from PYTHIA denoted  $d\sigma(had)/dp_T$  (the dotted histogram) is either equal or larger than  $d\sigma(NLO)/dp_T$ , so that



for most of the  $p_T$ -bins the PYTHIA correction dominates the experimental cross-section.

We have checked that our results do not depend on the choice of the NLO PDF MSTW. For this purpose we have replaced the MSTW PDF by the NLO Ct14 [14] and NLO MMHT [15] PDFs. We did not repeat all the calculations of cross sections as shown in Fig. 1, 2 and 3 for MSTW. We calculated only the LO cross-sections as shown in Fig. 1 (left frame) and the K-factor in Fig.1 (right frame). For the latter we needed also the NLO cross-sections. These four cross-sections were calculated with the same choice of scales as for the MSTW PDF described above. The results for the other two PDFs differed only by a few percent. Of course the LO cross-sections differed somewhat less than the NLO cross sections needed for the K-factor. This K-factor for the CT14 and MMHT PDFs showed the same behaviour as for the MSTW PDF in Fig 1 (right side). In particular  $K \simeq 1$  for the five  $p_T$  bins as in Fig 1 (right frame). These calculations have been done only for the larger  $\sqrt{S} = 5.02$  TeV. We expect very similar results for the lower  $\sqrt{S}$  value. Of course we can expect that our results in Fig. 2 and 3 (right side) will look similar for the CT14 and MMHT PDFs if the same choice of scales as for the MSTW PDF will be assumed.

A quite similar study has been done in our earlier work [4] on single bottom jets and for the MSTW PDF. Also in this case we obtained rather good agreement between CMS data at  $\sqrt{s} = 7$  TeV and in two rapidity ranges  $|y| \leq 0.5$  and  $0.5 \leq |y| \leq 1.0$  after correcting the calculated NLO cross-section  $d\sigma/dp_T$  with  $d\sigma(had)/dp_T$  as calculated in the charm case from the PYTHIA prediction which gave a reasonable description of the experimental CMS single-bottom jet cross section for  $p_T \geq 50$  GeV shown in [21]. Also in the bottom case the PYTHIA corrections yielded the largest part to the measured cross section. The K factor ( $K = d\sigma(NLO)/d\sigma(LO)$ ) was also calculated in Ref.[4], but only for the CDF energy  $\sqrt{S} = 1.96$  TeV for  $p\bar{p} \rightarrow b - jet + X$  and for  $|y| \leq 0.7$ . It came out as  $K \simeq 1.0$  but varying as a function of  $p_T$  in the region  $50 \leq p_T \leq 400$  GeV between  $0.5 < K < 1.3$ . We expect similar results for  $pp$  collisions at  $\sqrt{S} = 7$  and 13 TeV.

It seems that the hadronic corrections in the PYTHIA predictions account only for a moderate correction to the NLO cross section, so that the major part must originate from the parton-shower corrections. This has been confirmed in a more recent analysis of inclusive b-jet production cross-sections measured by the CMS collaboration at  $\sqrt{S} = 13$  TeV described in the thesis by P. Connor [22]. His work is based on CMS measurements of b jets in the  $p_T$  range from  $p_T = 74$  GeV to 1 TeV for several rapidity bins in the range from  $-2.4$

to +2.4. These data have much higher statistics than the earlier CMS and ATLAS b-jet measurements. He compared the b-jet cross-sections from the analysis of the more recent CMS data with two theoretical approaches, a LO routine with PYTHIA 8.1 corrections, which contains also parton-shower and parton-hadron corrections as the earlier PYTHIA Monte-Carlo programs. The second approach he compares the data to is a NLO routine with PYTHIA 8.1 corrections, denoted POWHEG [24]. Both routines give very good agreement with the new CMS data. This shows in particular, that for the single b-jet production in LO and NLO the parton-shower contributions are very important in contrast to the single inclusive jet-production of light quark flavours where this is not the case. In Ref. [22] it is demonstrated explicitly, that the parton-shower in PYTHIA dominates the b-jet production and the so-called hadronic corrections in PYTHIA are of minor importance. The reason for this difference between light-quark and b-jets is attributed to the fact that in b-jet production the LO process is already dominated by the gluon-splitting production into  $b\bar{b}$ . This is not the case in light-quark production, which is dominated by other LO processes.

We assume that the parton shower corrections are also dominant in the case of the charm-jet production similar to the bottom-jet production, although this was not explicitly investigated in Ref. [22]. For both cases, c-jet and b-jet, the question arises whether the main part of the parton shower corrections comes from the NNLO contributions of the parton shower or whether even higher parton showers or the whole sum is needed to obtain the whole PYTHIA corrections. In the latter case this would mean that the heavy-quark jet cross-sections can not be calculated by perturbative fixed-order QCD.

It is clear, that our approach contains an inconsistency with respect to the NLO corrections. On the one hand they are contained in the full NLO corrections calculated by us and on the second hand they are contained in the PYTHIA corrections in the parton shower approximations. This problem has been investigated by Connor in his thesis for the case of single inclusive b-jet production [22] by comparing the CMS data with the NLO POWHEG [24] routine showing as good agreement as for the pure PYTHIA comparison. We expect a similar agreement between these two approaches in the case of c-jet production.

As a final point we mention that the ALICE collaboration has also measured c-jet production in  $pp$  collisions at  $\sqrt{S} = 7$  TeV at the LHC [25]. The charm jets were identified by the presence of a  $D^0$  meson among the constituents of the jet with the constraint  $p_{T,D} > 3$  GeV. The  $D^0$ -meson tagged jets are reconstructed using tracks of charged particles only.

Due to these additional constraints it is unclear how they can be incorporated into the analytical calculations of the NLO calculation. Therefore we did not attempt to compare our calculations with the ALICE data.

#### IV. SUMMARY AND CONCLUSIONS

We have calculated the inclusive charm-jet cross section at NLO of QCD in the ZM-VFN scheme, i. e. with active charm quarks in the proton at  $\sqrt{S} = 2.76$  and  $\sqrt{S} = 5.02$  TeV for  $pp$  collisions at the LHC. The charm quarks are considered massless. Our results are compared to experimental jet cross section measurements by the CMS collaboration at the LHC. To our surprise the NLO cross sections are much smaller than the measured cross sections. They are for the considered  $p_T$  almost equal to the LO cross section, i. e. the K factor is approximately equal to one. There exist several possibilities to increase this contribution. Examples are: contributions originating from intrinsic charm-quark contributions to the proton PDF, as has been calculated in [3] or contributions from higher orders than NLO from QCD, which may become known in the future. This approach has been followed in this work by approximating these higher order corrections by parton shower corrections as contained in the PYTHIA Monte Carlo routines [19]. It turns out, similar to the results for b-jet production presented in [4], if the PYTHIA predictions minus the LO perturbative cross section is added to the calculated NLO predictions reasonable agreement with the measured c-jet cross sections can be achieved for CMS for both center of mass energies. In this connection the question arises whether this mechanism might be applicable also for other processes involving heavy quarks, charm or bottom, as for example,  $pp \rightarrow c - jet + \gamma + X$  or  $pp \rightarrow c - jet + Z + X$ . It is well known that the measurements of the first of these two examples is not in agreement with NLO predictions [26].

- 
- [1] S. Frixione, M.L. Mangano, P. Nason et al., Adv. Ser. Direct High Energy Phys. 15 (1998) 609; arXiv: hep-ph/9702287
- [2] S. Frixione and M.L. Mangano, Nucl. Phys. B483 (1997) 321 arXiv: hep-ph/9605270
- [3] I. Bierenbaum and G. Kramer, Int. J. Mod. Phys. A30 (2015) 1550111 arXiv:1412.5470 [hep-ph]

- [4] I. Bierenbaum and G. Kramer, *Int. J. Mod. Phys. A*31 (2016), 1650098, arXiv:1603.01138 [hep-ph]
- [5] CDF and D0 Collaborations (M. D’Onofrio), arXiv:0505036 [hep-ex]
- [6] CDF and DO Collaborations (M. D’Onofrio) FERMILAB-CONF-06-224E
- [7] CDF Collaboration, CDF Note 8418, July 25, 2006
- [8] S. Chatrchyan et al., CMS Collaboration, *J. High Energy Phys.*1204 (2012) 084, arXiv:1202.4617 [hep-ex]
- [9] G. Aad et al. ATLAS Collaboration, *Eur. Phys. J C*71 (2011) 1846, arXiv:1109.6833 [hep-ex]
- [10] A.M. Sirunyan et al., CMS Collaboration, *Phys. Lett. B*772 (2017), 306, arXiv:1612.08972 [nucl-ex]
- [11] M. Klasen and G. Kramer, *Z. Phys. C*72 (1996) 107, arXiv: hep-ph/9511405
- [12] M. Klasen and G. Kramer, *Z. Phys. C*76 (1997) 67, arXiv: hep-ph/9611450
- [13] A.D. Martin, W.J. Stirling, R.S. Thorne and G. Watt, *Eur. Phys. J. C*63 (2009) 189, arXiv: 0901,0002 [hep-ph]
- [14] S. Dulat et al., *Phys. Rev D*93 (2016) 033006, arXiv:1506.07443 [hep-ph]
- [15] L. A. Harland-Lang, A. D. Martin, P. Motylinski and R. S. Thorn, *Eur. Phys. J C*75 (2015) 204, arXiv:1412.3989 [hep-ph]
- [16] S. Chatrchyan et al., CMS Collaboration, *Phys. Rev. Lett.* 107 (2011), 132001, arXiv: 1106,0208 [hep-ex]
- [17] [http://hep.data.cedar.ac.uk/view/ins\\_902309](http://hep.data.cedar.ac.uk/view/ins_902309)
- [18] H.L. Lai et al., *Phys. Rev. D*82 (2010) 074024, arXiv: 1007.2241 [hep-ex]
- [19] T. Sjöstrand, S. Mrenna and P. Skands, *J. High Energy Phys.* 05 (2006) 026, arXiv: hep-ph 0603175
- [20] R. Field, *Acta Phys. Pol. B*42 (2011) 2631, arXiv:1110.5530 [hep-ph]
- [21] S. Chatrchyan et al., CMS Collaboration, *J. High Energy Phys.*, 1204 (2012) 084, arXiv: 1202.4617 [hep-ex]
- [22] P. Connor, DESY-THESIS-2018-016
- [23] T. Sjöstrand, S. Mrenna and P. Skands, *Comp. Phys. Comm.* 178 (2008) 852
- [24] S. Alioli et al., *J. High Energy Phys.* 1104 (2011) 081, arXiv:10122380 [hep-ph]
- [25] S. Acharya et al., ALICE Collaboration, *J. High Energy Phys.*, 1808 (2019) 133, arXiv: 1905.02510 [hep-ex]

[26] V. M. Abazov, et al., D0 collaboration, Phys. Lett. B719 (2013) 354, arXiv: 1210.5033 [hep-ex]

